IEEE Access
Multidisciplinary | Rapid Review | Open Access Journal

Received September 28, 2018, accepted October 24, 2018, date of publication November 9, 2018,
date of current version November 30, 2018.

Digital Object Identifier 10.1109/ACCESS.2018.2879012

Application of Pulse Compression Technique in Fault Detection and Localization of Leaky Coaxial Cable

YANG LIU[1], YANNAN SHI[2], JINXI GUO[2], AND YIYING WANG[2]
[1]School of Mechanical Electronic & Information Engineering, China University of Mining and Technology (Beijing), Beijing 100083, China
[2]College of Mechanical and Equipment Engineering, Hebei University of Engineering, Handan 056038, China

Corresponding author: Yannan Shi (shiynchn@163.com)

This work was supported in part by the National Natural Science Foundation of China under Grant 51604279 and in part by the Hebei Province Higher Education Science and Technology Research Project under Grant QN2018093.

ABSTRACT In this paper, an efficient technique in fault detection and localization of leaky coaxial cable (LCX) is presented. The approach utilizes a high-resolution reflectometry technique, which injects a reference signal into an LCX and handles the reflected signal to locate the fault. The reference signal adopts a linear frequency modulation signal by an approximately rectangular magnitude spectrum, which can ensure that the detection distance is large enough. And the pulse compression technique is used to improve the resolution of the reflected signal. Therefore, the approach can solve the contradiction between the detection distance and the high-resolution. The proposed method is verified by detecting various types of faults at different distances in MSLYFYVZ-50-9 LCX.

INDEX TERMS Linear frequency modulation (LFM), pulse compression, leaky coaxial cable (LCX), fault detection, fault localization.

I. INTRODUCTION

In recent years, the most rapidly developing and widely used in the field of information and communication is wireless communication technology [1]–[5]. At present, the frequency band of LCX covers 450 MHz $\sim$ 2.4 GHz, which is suitable for various existing wireless communication systems. And it is widely used in many fields such as coal mine, subway, vehicular technology, et al [6]–[8]. Its structure is similar to that of the common coaxial cable. As LCX aging, it is subjected to several stresses (e.g. electrical, chemical and mechanical) that lead to cracks, abrasions, breaks, loose connection, and other damages. This has a serious impact on the normal work and production. Thus, the detection and localization of faults on an LCX have become a critical issue.

At present, there is seldom approach to detect and locate a fault on an LCX. But we can learn from the methods in fault detection and localization of other cables. Partial discharge (PD) is mentioned to detect and locate faults in extruded power cables [9], [10]. However, this method has limitations in the practical application, which is easily influenced by noise. Until now, reflectometry is a widely used method in fault detection and localization of cables [11]. The basic principle of reflectometry is to inject a reference signal into the cable, and the reflected signal will be generated when the reference signal encounters the impedance discontinuity. The fault of the cable can be located according to the difference between the reference signal and the reflected signal.

The fault detection of the cable based on reflectometry is categorized into time domain analysis and frequency domain analysis, which correspond to time-domain reflectometry (TDR) [12] and frequency-domain reflectometry (FDR). Reference [13] proposes to detect faults in wiring networks from TDR response. Reference [14] adopts a low-cost FDR to test the integrity of aircraft cables nondestructively on board. And Reference [15] applies phase detection FDR to locate faults in an F-18 flight control harness. However, the accuracy and resolution of the above methods are limited by the frequency sweep bandwidth and rise/fall time, respectively. In addition, sequence time domain reflectometry (STDR), and spread sequence time domain reflectometry (SSTDR) are examined as potential solutions to the difficult problem of locating intermittent faults on aircraft wires with typical signals in flight [16]. A fault detection and localization of coaxial cable based on time-frequency domain reflectometry (TFDR) is proposed in [17]. However, above-mentioned methods suffer from a contradiction between the detection distance and high-resolution. So the frequency division multiplexed (FDR) signal is presented to

detect faults based on TFDR [18]. Although this approach can optimize the relationship between the detection distance and high-resolution, it is difficult to acquire parameters in fault detection.

The novelty of this paper is to introduce a reflectometry in fault detection and localization of LCX based on pulse compression technique. It is based on the same principle as radar. To detect further distance, the reference signal is an LFM signal which has an approximately rectangular magnitude spectrum. To improve the resolution for fault detection, the pulse compression technique is applied to handle the reflected signals. The injection into the LCX of LFM signal for fault localization based on pulse compression technique represents a new application.

The structure of this paper is as the following. In Section II, the fundamental idea of LFM pulse compression is discussed. In Section III, several experiments are carried out and compared with the ability of TDR and LFM pulse compression when different types of faults occur at different distances in the LCX. In Section IV, the result and analysis are presented. The conclusions of these experimental results are obtained in Section V.

II. LFM PULSE COMPRESSION

In the fault detection of the LCX, if the LCX is normal, the reference signal will be absorbed by the load and no reflected signal will be generated according to the transmission line theory. If the LCX has an open-type fault, a reflected signal with the same amplitude and polarity as the reference signal will be generated. If the LCX has a short-type fault, a reflected signal with the same amplitude and the opposite polarity of the reference signal will be generated.

A. DESIGN OF REFERENCE SIGNAL

When fault detection and localization are carried out, the detection distance of the reference signal rests with its width. The resolution relies on the width of the reflected signal. Since wider pulse allows longer detection distance but suffers lower resolution, we must consider a balance between the detection distance and the high-resolution. In view of this, this paper proposes an LFM pulse compression technique for the fault detection of the LCX, which can ensure enough detection distance and improve the resolution [19].

The reference signal is represented as,

$$s(t) = A rect(\frac{t}{\tau}) e^{j2\pi(f_0 t + \frac{Bt^2}{2\tau})}, \tag{1}$$

where A, B, f_0, τ determine the amplitude, frequency bandwidth, center frequency, and time duration, respectively. $rect(t/\tau)$ is rectangular function, whose expression is,

$$rect\frac{t}{\tau} = \begin{cases} 1, & \left|\frac{t}{\tau}\right| \le 1 \\ 0, & \text{otherwise.} \end{cases} \tag{2}$$

To apply the LFM signal to the fault detection of the LCX, the attenuation characteristics of the LCX and the performance of the experimental instruments should be considered when selecting parameters. The steps of parameters selection are as follows [17]:

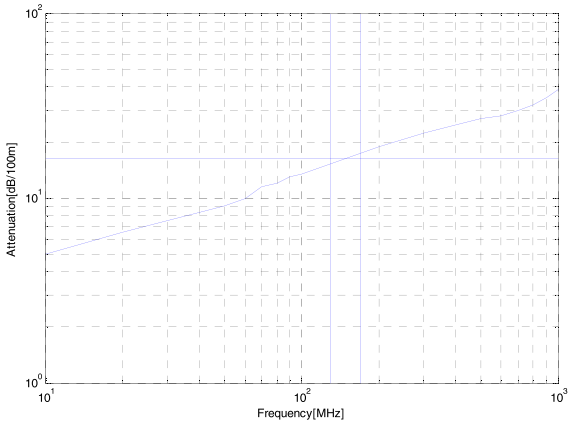

FIGURE 1. Frequency-dependent attenuation characteristic of the LCX in dB per 100 m.

(1) The center frequency is determined according to the attenuation degree of the LFM signal through the LCX. Because the higher the frequency is, the higher the resolution power. And the attenuation degree of the signal will increase. In this experiment, the maximum fault distance setting is 130 m. The maximum signal attenuation that we can tolerate is 16.5 dB/100 m. Frequency-dependent attenuation characteristic of the LCX in dB per 100 m is shown in Fig. 1.

As can be seen from Fig. 1, the horizontal line of 16.5 dB/100 m is about 150 MHz at the intersection of the attenuation curve, so we select 150 MHz as the center frequency of the LFM signal.

(2) The frequency bandwidth of the LFM signal depends on the performance of the signal generator and the circulator. We select 40 MHz as the frequency bandwidth of the LFM signal. So the frequency range of interest is selected as 130 MHz $\sim$ 170 MHz. The initial frequency of the LFM signal is 130 MHz, and the cut-off frequency is 170MHz.

(3) According to the performance of the signal generator and the selection of the parameters above, we select 10 μs as the time duration of the LFM signal.

In summary, in this paper, the parameters of the LFM signal are as follows:

- Center frequency: $f_0 = 150$ MHz
- Frequency bandwidth: $B = 40$ MHz
- Time duration: $\tau = 10$ μs

The Fourier transform of the LFM signal in (1) is obtained as,

$$S(\omega) = A\sqrt{\frac{\pi}{\mu}} \left\{ [c(\nu_1) + c(\nu_2)]^2 + [s(\nu_1) + s(\nu_2)]^2 \right\}^{\frac{1}{2}} \cdot e^{j\left[\frac{1}{2\mu}(\omega-\omega_0)^2 + \arctan\frac{s(\nu_1)+s(\nu_2)}{c(\nu_1)+c(\nu_2)}\right]}, \tag{3}$$

where $c(v)$, $s(v)$, v_1, v_2 and μ can be evaluated as the following,

$$c(v) = \int_0^v \cos(\frac{\pi}{2}x^2)dx, \tag{4}$$

$$s(v) = \int_0^v \sin(\frac{\pi}{2}x^2)dx, \tag{5}$$

$$v_1 = \frac{\mu\pi/2 + (\omega - \omega_0)}{\sqrt{\mu\pi}}, \tag{6}$$

$$v_2 = \frac{\mu\pi/2 - (\omega - \omega_0)}{\sqrt{\mu\pi}}, \tag{7}$$

$$\mu = \frac{2\pi\,\Delta f}{\tau}, \tag{8}$$

where $c(v)$ and $s(v)$ are the final integrals and their values can be found on the specialized function table. Δf is the modulation frequency deviation and its value is equal to B. w_0 is center angle frequency, μ is modulation slope. x in (4) and (5) is given by,

$$x = \sqrt{\frac{\pi}{\mu}}(t - \frac{\omega - \omega_0}{\mu}). \tag{9}$$

According to (3), the amplitude spectrum and phase spectrum of the reference signal can be evaluated as the following,

$$|S(\omega)| = A\sqrt{\pi/\mu}\left\{[c(v_1) + c(v_2)]^2 + [s(v_1) + s(v_2)]^2\right\}^{1/2}, \tag{10}$$

$$\phi(\omega) = -\frac{(\omega - \omega_0)^2}{2\mu} + \arctan\frac{S(v_1) + S(v_2)}{C(v_1) + C(v_2)}. \tag{11}$$

When the time bandwidth product is much larger than 1 (namely $\tau B \gg 1$), the (10) and (11) can be expressed as the following,

$$|S(\omega)| = \begin{cases} A\sqrt{2\pi/\mu}, & |\omega - \omega_0| \le \Delta\omega/2 \\ 0, & |\omega - \omega_0| > \Delta\omega/2, \end{cases} \tag{12}$$

$$\phi(\omega) = -\frac{(\omega - \omega_0)^2}{2\mu} + \frac{\pi}{4}, \quad |\omega - \omega_0| \le \Delta\omega/2. \tag{13}$$

The sampling rate is 2 times of the frequency bandwidth. According to (1), (12) and (13), the real part, magnitude spectrum and phase spectrum of the LFM signal are shown in Fig. 2.

From Fig. 2, we see that the LFM signal has an approximately rectangular magnitude spectrum, in the range of B, which is relatively flat. And the signal energy is mainly concentrated in this range. Therefore, it can ensure the reference signal has a large enough traveling distance in the LCX. Meanwhile, the LFM signal has a square-law phase spectrum, which is the main consideration in designing the matched filter.

B. DESIGN OF MATCHED FILTER

The matched filter is designed to achieve the purpose of pulse compression and improve the Signal-Noise Ratio (S/N) by processing the LFM signal and the reflected signal. When the

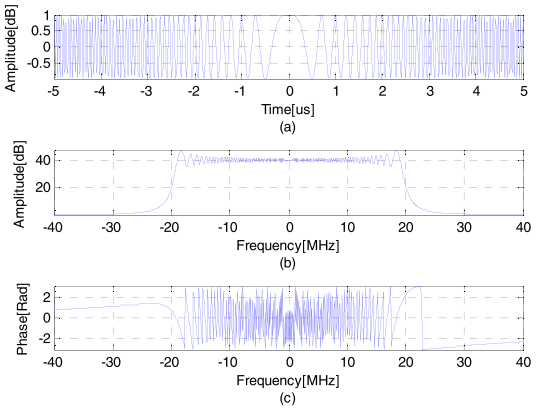

FIGURE 2. (a) Real part, (b) magnitude spectrum, (c) phase spectrum, of LFM signal.

S/N gets the maximum value, the frequency characteristic of the matched filter should satisfy the following relations,

$$H_r(\omega) = G\,|S(\omega)|\,e^{-j\phi(\omega)}e^{-j\omega t_{d0}}, \tag{14}$$

where t_{d0} is the additional delay for the physical implementation of the matched filter.

According to (12) and (13), the amplitude spectrum and phase spectrum of the matched filter can be expressed as follows,

$$|H_r(\omega)| = \begin{cases} GA\sqrt{2\pi/\mu}, & |\omega - \omega_0| \le \Delta\omega/2 \\ 0, & |\omega - \omega_0| > \Delta\omega/2, \end{cases} \tag{15}$$

$$\phi_r(\omega) = \frac{(\omega - \omega_0)^2}{2\mu} - \frac{\pi}{4} - \omega t_{d0}, \quad |\omega - \omega_0| \le \Delta\omega/2. \tag{16}$$

In order to facilitate the analysis, G is the normalized coefficient. And G in (14) and (15) are given by,

$$G = \frac{\sqrt{\mu/2\pi}}{A}. \tag{17}$$

According to (15), (16) and (17), the frequency characteristic of the matched filter can be expressed as,

$$H_r(\omega) = e^{j\frac{(\omega-\omega_0)^2}{2\mu} - \frac{\pi}{4} - \omega t_{d0}}, |\omega - \omega_0| \le \Delta\omega/2. \tag{18}$$

Thus, the matched filter has an approximately rectangular magnitude spectrum. And the matched filter has a square-law phase spectrum, which is the same as the LFM signal but opposite to the sign. The frequency characteristic of the LFM signal after matched filter can be given as,

$$S_o(\omega) = S(\omega)H_r(\omega). \tag{19}$$

According to (3) and (18), the inverse Fourier transform of the (19) is obtained as,

$$s_o(t) = \frac{A\Delta\omega}{2\pi}\sqrt{\frac{2\pi}{\mu}}\frac{\sin[\Delta\omega(t - t_{d0})/2]}{\Delta\omega(t - t_{d0})/2}e^{jw_0(t-t_{d0})}. \tag{20}$$

Substituting $\Delta\omega = 2\pi B$, $\mu = 2\pi B/\tau$, $\omega_0 = 2\pi f_0$ in (20), then obtaining the real part as,

$$s_o(t) = A\sqrt{D}\frac{\sin[\pi B(t - t_{d0})]}{\pi B(t - t_{d0})}\cos 2\pi f_0(t - t_{d0}), \quad (21)$$

where D is the pulse compression ratio, which is equal to the time bandwidth product of the LFM signal.

According to (21), it can be seen that the output signal has the form of sinc function. Usually the width at 4 dB under the vertex is defined as the out pulse width, which is approximately the reciprocal of the bandwidth of the LFM signal (namely $\tau_0 = 1/B$). Also, the out pulse width is D times smaller than the input pulse width, that is, the amplitude of the output pulse is $\sqrt{D}$ times larger than the amplitude of the input pulse. In addition, the carrier frequency of the output signal is single frequency f_0.

The sampling rate is 10 times of the frequency bandwidth. Simulation and theoretical results of the LFM signal after the matched filter are shown in Fig. 3 based on the selected parameters.

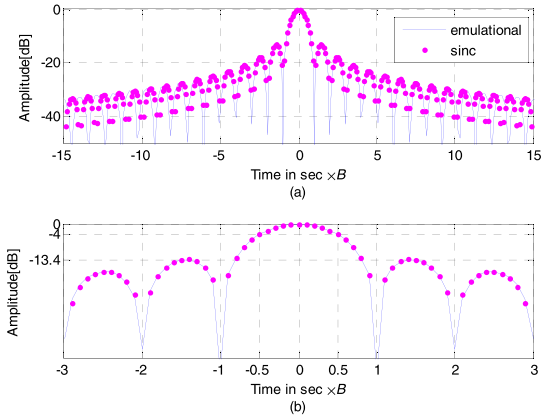

FIGURE 3. (a) LFM signal after matched filter and (b) LFM signal after matched filter (Zoom).

In Fig. 3, we see that first zero occurs at ± 1 (namely $\pm 1/B$), when the relative amplitude is -13.4 dB. The width of the LFM signal after the matched filter is $1/B$, when the relative amplitude is -4 dB. Through the theoretical analysis of the LFM signal, we can know that the pulse compression ratio is equal to the time-bandwidth product of the LFM signal. It shows that the LFM signal has excellent pulse compression performance, and it can solve the contradiction between the detection distance and the high-resolution.

III. EXPERIMENTAL SETUP

To verify the feasibility of the LFM pulse compression in fault detection and localization of LCX, an experimental platform is designed as Fig. 4.

In Fig. 4, we see that the experimental system consists of a signal generator (R&S, SMW200A), a digital oscilloscope (R&S, RTO2044), a spectrum analyzer (R&S, FSW), a computer, and an LCX (MSLYFYVZ-50-9). The signal generator produces the LFM signal, which is transmitted to the LCX through the circulator. The LFM signal is emitted and back

FIGURE 4. Experimental setup for fault detection.

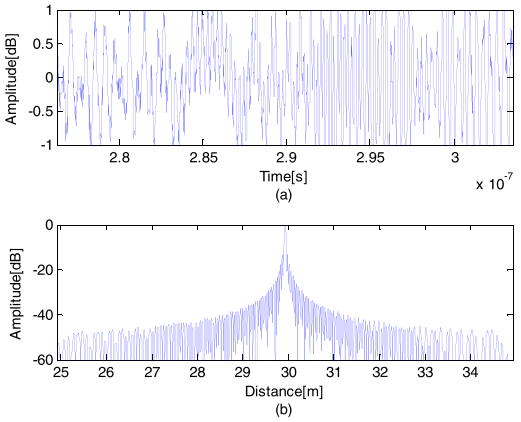

FIGURE 5. Reflected signal in (a) and pulse compression for localization the open fault in (b) at 30 m in the LCX.

to the circulator when encountering impedance discontinuity. The circulator redirects the reflected signal to the digital oscilloscope. The computer carries on the data processing to the reflected signal and executes the pulse compression algorithm. It is necessary to point out that the spectrum analyzer in Fig. 4 only plays the role of the spectrum analysis of the signal generated by the signal generator, and does not affect the experimental results.

Next, the performance is to be compared with TDR. A total of 10 experiments are carried out for different distances and types of faults. The actual fault distances are 10, 20, 30, 120, and 130 m, while the types of faults are classified as ''open'' and ''short''. Then, other 10 experiments are repeated by using a commercial TDR method for comparison purposes.

IV. RESULT AND ANALYSIS

In the previous section, we have done several fault detection and localization experiments to verify the feasibility and evaluate the performance of the LFM pulse compression. Meanwhile, we used the same velocity of propagation, $v = 2.1 \times 10^8$ m/sec., when calculating the fault distance [17].

A. EXPERIMENTAL RESULT

We take the LCX which has an open-type fault located at 30 meters away from the starting point as the first example. Fig. 5 presents the acquired time series of the reflected signal

at a 200 MHz sampling rate. In Fig. 5(a), the reflected signal is accompanied by a noise signal and it is difficult to read. In Fig. 5(b), the reflected signal after pulse compression has a high peak value and S/N. And we can see the location of the fault, and its estimated distance is 29.82 m.

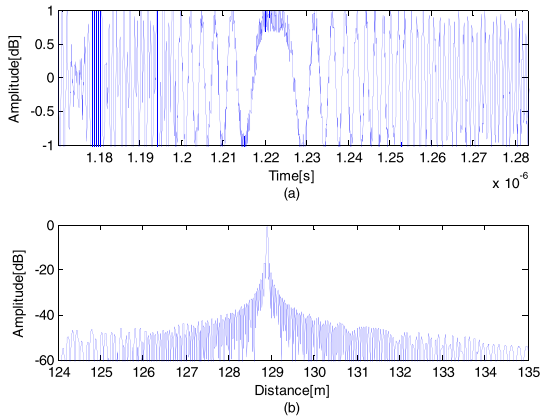

FIGURE 6. Reflected signal in (a) and pulse compression for localization the open fault in (b) at 130 m in the LCX.

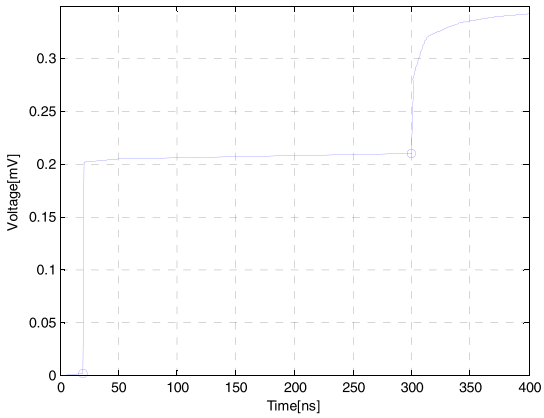

FIGURE 7. Reflected signal based on TDR.

The second example shown in Fig. 6 illustrates a case for the LCX which has an open-type fault located at 130 meters away from the starting point. In Fig. 6(a), the reflected signal is accompanied by a noise signal. Compared with Fig. 5(a), it is also difficult to read. In Fig. 6(b), however, we can clearly see the location of the fault, and its estimated distance is 128.78 m.

In order to compare it with the previous methods, an experiment based on the TDR using the same LCX with an open-type fault located at 30 meters away from the starting point is carried out. Fig. 7 presents the reflected signal based on TDR at a 12 GHz sampling rate. As shown in Fig. 7, the estimated time points of the step changes of the reflected signal are 20 ns and 300.38 ns. Therefore, we can acquire that the estimated distance of the location of the fault is 29.44 m.

B. ANALYSIS AND DISCUSSION OF RESULTS

In order to compare the performances of LFM pulse compression and TDR, fault distances range from 10, 20, 30, 120, to 130 m and two types of faults are tested in each distance. The results of the experiments are shown in Table 1. The locating errors of LFM pulse compression vary from 0.09 m to 1.43 m while that of TDR range from 0.48 m to 4.77 m. Compared with TDR, the method proposed in this paper has more accuracy in all cases. For that reason, there is much greater accuracy in further distance.

TABLE 1. The results of the experiment.

	fault type	LFM pulse compression	error (m)	TDR	error (m)
10 m	open	9.91	0.09	9.52	0.48
	short	9.88	0.12	9.52	0.48
20 m	open	19.82	0.18	19.45	0.55
	short	19.85	0.15	19.38	0.62
30 m	open	29.82	0.18	29.44	0.56
	short	29.78	0.22	29.31	0.69
120 m	open	118.68	1.32	116.57	3.43
	short	118.57	1.43	116.84	3.16
130 m	open	128.78	1.22	125.23	4.77
	short	128.63	1.37	125.36	4.64

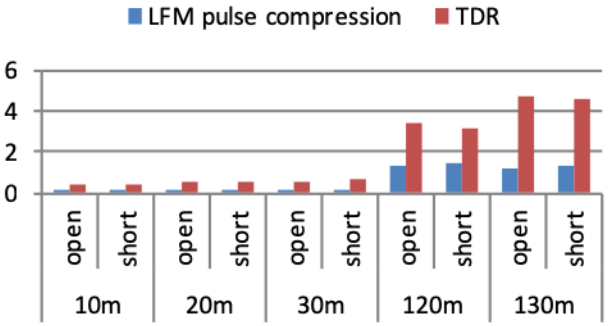

FIGURE 8. Error comparison for LFM pulse compression and TDR.

To observe the experimental results more intuitively, the locating error comparison of LFM pulse compression and TDR is shown in Fig. 8.

In Fig. 8, we can see more intuitively that LFM pulse compression has a smaller locating error than TDR in all cases. As the fault distance increases, the locating errors of the two methods are getting larger. But LFM pulse compression shows a better performance. It optimizes the trade-off relationship between the detection distance and the high-resolution. The experimental results suggest that LFM pulse compression has a much better performance than TDR in fault detection and localization of the LCX.

V. CONCLUSION

This paper described an efficient reflectometry method in fault detection and localization of LCX. This approach uses the LFM signal as the reference signal and carries on the pulse compression to the reflected signal from the fault. The experimental work involving five fault lengths and two types of faults indicates that LFM pulse compression makes a better performance than TDR in fault detection and localization with long distance and high-resolution. The contributions of the pulse compression technique are as the following:

(1) Accurate and sensitive detection and distinction of the reflected signal.

(2) Successful detection and localization of fault on the LCX, even in further distance.

(3) Solving the contradiction between the detection distance and the high-resolution on the basis of ensuring the accuracy of fault detection.

Clearly, there is a lot of work to do in the future, including consideration of more complex noise; a detailed comparison with other reflectometry methods; and the identification of the advantages and disadvantages of pulse compression technique.

REFERENCES

[1] H. Hassan *et al.*, "H.264 encoder parameter optimization for encoded wireless multimedia transmissions," *IEEE Access*, vol. 6, pp. 22046–22053, Apr. 2018.
[2] M. H. Malik, M. Jamil, M. N. Khan, and M. H. Malik, "Formal modelling of TCP congestion control mechanisms ECN/RED and SAP-LAW in the presence of UDP traffic," *Eurasip J. Wireless Commun. Netw.*, vol. 2016, no. 1, pp. 1–12, Dec. 2016.
[3] Y. Hou, S. Tsukamoto, S. Li, T. Higashino, K. Kobayashi, and M. Okada, "Capacity evaluation of MIMO channel with one leaky coaxial cable used as two antennas over linear-cell environments," *IEEE Trans. Veh. Technol.*, vol. 66, no. 6, pp. 4636–4646, Jun. 2017.
[4] M. N. Khan *et al.*, "Maximizing throughput of hybrid FSO-RF communication system: An algorithm," *IEEE Access*, vol. 6, pp. 30039–30048, May 2018.
[5] M. N. Khan, M. Jamil, and M. Hussain, "Adaptation of hybrid FSO/RF communication system using puncturing technique," *Radioengineering*, vol. 25, no. 4, pp. 12–19, Dec. 2016.
[6] N. Nakamura, H. Tsunomachi, and R. Fukui, "Road vehicle communication system for vehicle control using leaky coaxial cable," *IEEE Commun. Mag.*, vol. 34, no. 10, pp. 84–89, Oct. 1996.
[7] L. Feng, X. Yang, Z. Wang, and Q. Yang, "Application of leaky coaxial cable in subway mobile communication system," in *Proc. Cross Strait Quad-Regional Radio Sci. Wireless Technol. Conf. (CSQRWC)*, Jul. 2011, pp. 119–122.
[8] Y. Shi, J. Liu, Z. Liu, and S. Li, "Study on modeling method of leaky coaxial cable network channel in underground coal mine," in *Proc. IEEE 17th Int. Conf. Commun. Technol.*, Oct. 2017, pp. 160–164.
[9] S. M. Miri and A. Privette, "A survey of incipient fault detection and location techniques for extruded shielded power cables," in *Proc. 26th Southeastern Symp. Syst. Theory*, Athens, OH, USA, Mar. 1994, pp. 402–405.
[10] M. Tozzi, A. Cavallini, G. C. Montanari, and G. L. G. Burbui, "PD detection in extruded power cables: An approximate propagation model," *IEEE Trans. Dielectr. Electr. Insul.*, vol. 15, no. 3, pp. 832–840, Jun. 2008.
[11] C. Furse, Y. C. Chung, C. Lo, and P. Pendayala, "A critical comparison of reflectometry methods for location of wiring faults," *Smart Struct. Syst.*, vol. 2, no. 1, pp. 25–46, 2006.
[12] C. Nemarich, "Time domain reflectometry liquid level sensors," *IEEE Instrum. Meas. Mag.*, vol. 4, no. 4, pp. 40–44, Dec. 2001.
[13] M. K. Smail, L. Pichon, M. Olivas, F. Auzanneau, and M. Lambert, "Detection of defects in wiring networks using time domain reflectometry," *IEEE Trans. Magn.*, vol. 46, no. 8, pp. 2998–3001, Aug. 2010.
[14] C. Furse, Y. C. Chung, R. Dangol, M. Nielsen, G. Mabey, and R. Woodward, "Frequency-domain reflectometry for on-board testing of aging aircraft wiring," *IEEE Trans. Electromagn. Compat.*, vol. 45, no. 2, pp. 306–315, May 2003.
[15] Y. C. Chung, C. Furse, and J. Pruitt, "Application of phase detection frequency domain reflectometry for locating faults in an F-18 flight control harness," *IEEE Trans. Electromagn. Compat.*, vol. 47, no. 2, pp. 327–334, May 2005.
[16] P. Smith, C. Furse, and J. Gunther, "Fault location on aircraft wiring using spread spectrum time domain reflectometry," *IEEE Sensors J.*, vol. 5, no. 6, pp. 1469–1478, Dec. 2005.
[17] Y.-J. Shin *et al.*, "Application of time-frequency domain reflectometry for detection and localization of a fault on a coaxial cable," *IEEE Trans. Instrum. Meas.*, vol. 54, no. 6, pp. 2493–2500, Dec. 2005.
[18] M. K. Jung, J. S. Yong, and B. P. Jin, "Application of time-frequency domain reflectometry based on multi-band signal for detection and localization of fault on cable," in *Proc. 14th Int. Conf. Control Automat. Syst.*, Seoul, South Korea, Oct. 2014, pp. 396–401.
[19] I. Intyas, R. Hasanah, M. R. Hidayat, B. Hasanah, A. B. Suskmono, and A. Munir, "Improvement of radar performance using LFM pulse compression technique," in *Proc. Int. Conf. Elect. Eng. Informat. (ICEEI)*, Denpasar, Indonesia, Aug. 2015, pp. 302–307.

YANG LIU was born in Xingtai, Hebei, China, in 1982. He received the Ph.D. degree in power electronics and power transmission from the China University of Mining and Technology, Xuzhou, China, in 2014. He is currently a Lecturer with the School of Mechanical Electronic & Information Engineering, China University of Mining and Technology (Beijing). His research interests include mine wireless communication and distribution system planning.

YANNAN SHI was born in Jiaozuo, Henan, China, in 1988. He received the M.S. degree in control science and engineering from Henan Polytechnic University, Jiaozuo, in 2015, and the Ph.D. degree in control theory and engineering from the China University of Mining and Technology (Beijing), Beijing, China, in 2018. His research interests include wireless communication and fault diagnosis.

JINXI GUO was born in Zhoukou, Henan, China, in 1988. He received the M.S. degree in mechanical design and theory from the Hebei University of Engineering, Handan, China, in 2014, and the Ph.D. degree in detection technology and automatic equipment from the China University of Mining and Technology (Beijing), Beijing, China, in 2018. His research interests include wireless communication and fault diagnosis.

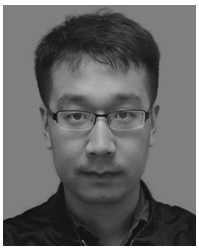

YIYING WANG was born in Baoding, Hebei, China, in 1985. He received the M.S. degree in computer science and technology from the Hebei University of Engineering, Handan, China, in 2009, and the Ph.D. degree in control theory and engineering from the China University of Mining and Technology (Beijing), Beijing, China, in 2017. His research interests include wireless communication and wireless sensor networks.